

# Properties of Hybrid Water/Gas DC Arc Plasma Torch

Milan Hrabovsky, *Member, IEEE*, Vladimir Kopecky, Viktor Sember, Tetyana Kavka, Oleksiy Chumak, and Milos Konrad

**Abstract**—A new type of plasma torch with combined stabilization of electric arc by water vortex and gas flow was investigated. This hybrid water/gas stabilization offers the possibility of adjusting plasma jet parameters within a wide range from high enthalpy, low density plasmas typical for liquid stabilized torches to lower enthalpy, higher density plasmas generated in gas stabilized torches. The torch was operated at a arc power from 22 kW to 130 kW with an exit centerline plasma velocity from 2 km/s to 6.5 km/s and a plasma temperature from 14 000 K to 22 000 K. Moreover, gas flow in the cathode part protects a cathode tip and thus a consumable carbon cathode used in water torches could be replaced by a fixed tungsten cathode. The characteristics of the electric arc with combined gas/water stabilization were measured and the effect of gas properties and flow rate on plasma properties and gas-dynamic flow characteristics of the plasma jet were studied for argon, and mixtures of argon with hydrogen and nitrogen.

**Index Terms**—Plasma torch, thermal plasma jet, water-stabilized arc, hybrid gas/water stabilization.

## I. INTRODUCTION

PLASMA jets generated in DC non-transferred arc torches are utilized in several plasma processing technologies such as, plasma spraying, plasma cutting, plasma synthesis and decomposition of persistent chemical substances. In commonly used plasma torches, the arc is stabilized by the gas flow along the arc column [1], [2]. Plasma jets with substantially different characteristics that cannot be achieved in gas torches are generated in arcs stabilized by a water vortex [3], [4]. Besides the apparent advantage of water-stabilized generators, namely, that no gas supply is needed because the plasma is produced by heating and ionizing steam evaporated from the stabilizing water vortex, there are many other differences between gas and water torches in plasma processes, plasma properties and especially in performance characteristics in plasma processing. Water torches are characterized by an extremely low plasma mass flow rates, and thus for the same arc power the plasma enthalpy is several

times higher than enthalpies achieved in common gas torches. The first measurements of properties of water stabilized arcs were published in the fifties [5]-[8], detailed experimental investigation of the water stabilized plasma torch and measurements of properties of generated plasma jets were performed during the last decade [3], [4], [9], [10]. The theoretical model of the water-stabilized arc is formulated in [11], [12]. Water torches have been industrially applied especially for plasma spraying [13].

The physical limits of the two principles, the gas and the liquid arc stabilization, do not allow generation of plasmas with parameters in a wide region between the two principles [14]. For some applications such as plasma spraying, where plasma jets are used to heat and accelerate the particles injected into the jet, the high enthalpy jets generated in water torches ensure a high level of efficiency of the particle heating and thus high throughputs, while low plasma flow rates and density result in lower efficiency of the particle acceleration [4]. Thus, it is desirable to create a plasma torch with thermal characteristics typical for the water torches but with increased plasma flow rates and densities. These ideas led to the development of the hybrid water/gas torch where principles of arc stabilization by gas flow and water vortex are combined. The hybrid torch is composed of two stabilizing chambers. Plasma produced in the cathode arc chamber with the gas stabilization enters the second chamber with the water stabilization.

This paper presents results of the experimental investigation of the water/gas stabilized arc and measurement of properties of the generated plasma jet. The effects of the gas composition and the flow rate on the arc characteristics and the plasma properties were studied. Measured characteristics were analyzed on the basis of the simple integral model of the arc. Physical processes that determine properties of the generated plasma are discussed.

## II. EXPERIMENTAL SET-UP AND TORCH CONFIGURATION

The plasma torch configuration and the schema of the experimental arrangement are shown in Fig. 1. The cathode part of the torch is arranged similar to gas torches. Gas is supplied along the cathode vortex component of the gas flow assures proper stabilization of the arc in the cathode nozzle. Plasma flows through the nozzle into the second part of the

Manuscript received July 18, 2005. This work was supported by the Grant Agency of the Czech Republic under Grant 202/05/0669.

The authors are with the Institute of Plasma Physics, Academy of Sciences of the Czech Republic, Prague 8, Za Slovankou 3, 182 00, Czech Republic (phone: +420-2-6605-3538; fax: +420-2-85686389; e-mail: hrabovsky@ipp.cas.cz).

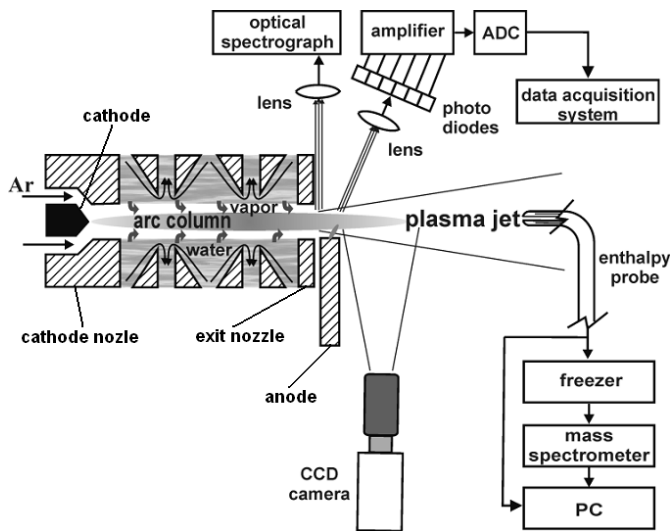


Fig. 1. Schematic of the plasma torch and experimental set-up.

torch where the arc column is surrounded by a water vortex. The vortex is formed in three cylindrical segments with a tangential water injection as it is in water-stabilized torches. The segments are separated by two exhaust gaps, where water is emptied from the arc chamber. Interaction of the arc column with the water vortex causes evaporation from the inner surface of the vortex. The steam mixes with the plasma flowing from the cathode section, and the overpressure produced in the arc chamber due to the evaporation accelerates the plasma, created by a mixture of steam and gas, towards the exit nozzle. The anode of the torch is created by a rotating copper disc that is located outside the arc chamber about 4 mm downstream of the exit nozzle. Both the cathode and anode have internal water cooling. The diameter of the exit nozzle was 5.7 mm.

The arc column is composed of three sections. The cathode section is stabilized by a vortex gas flow. The most important section is the water-stabilized part, where the arc column interacts with the water vortex. The third part between the exit nozzle and the anode attachment is an arc column in a free jet. The length of the gas-stabilized arc column was about 6 mm, and the length of the water-stabilized column was 50 mm. The length of the arc column in the free jet between the exit nozzle and the position of arc attachment varied from 4 to 24 mm as the anode attachment moved along the electrode surface in the re-strike mode [15].

Potentials of the electrodes, the cathode nozzle and the exit nozzle were measured by high resistance voltage dividers. From calorimetric measurements on cooling loops of the electrodes and of the water stabilizing system, the power loss to electrodes and to the stabilizing water vortex were determined. Volt-ampere characteristics and power balances of all parts of the arc were evaluated from these measurements.

Properties of the argon/steam plasma jet were investigated using several diagnostic methods. Profiles of plasma temperature and composition in several positions downstream

of the exit nozzle were determined by emission spectroscopy using the monochromator Jobin Yvon HR-320 equipped with a grating of 1200 grooves/mm and linear photodiode array detector of 1024 pixels. The apparatus function (FWHM) measured with a low-pressure mercury lamp at 491 nm was about 0.13 nm.

The electron number density was obtained from Stark broadened  $H_{\beta}$  line. To determine the plasma temperature and composition, a variety of atomic and ionic lines of different species were recorded in several spectral regions. The temperature was calculated from the ratios of diverse argon atomic to ionic line emission coefficients by using the Saha

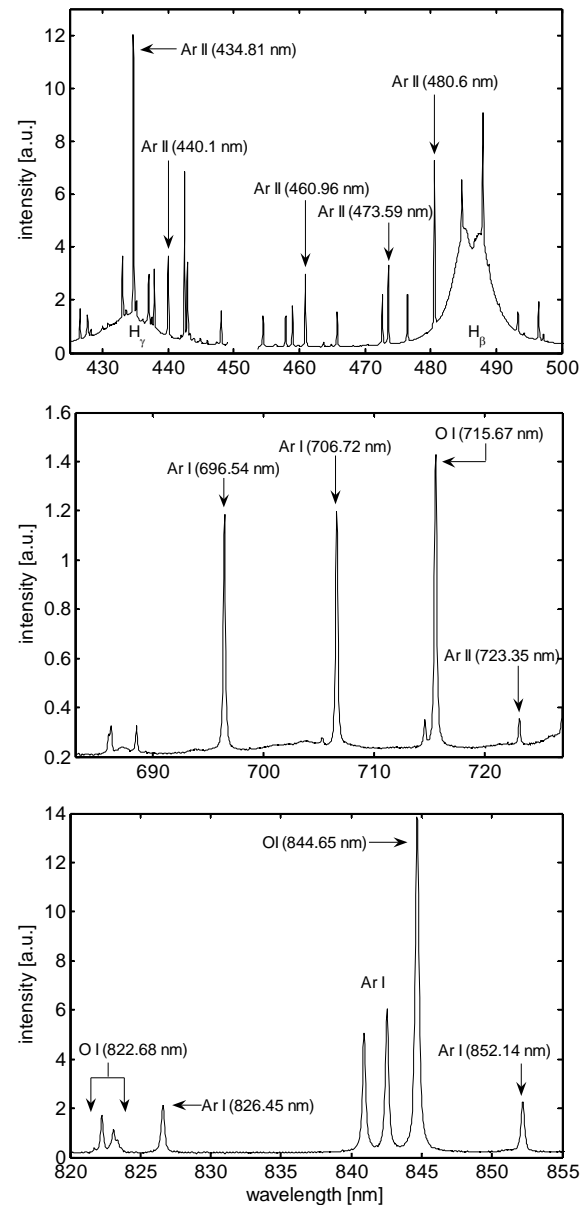


Fig. 2. Optical emission spectrum at the nozzle exit for arc current 400 A and argon flow rate 22.5 slm.

equation and the measured electron number density. The spectrum with the lines used for evaluation of plasma

properties is shown in Fig. 2. In colder parts, where no ionic lines were detected, the temperature was estimated from the approximate LTE composition and measured electron number density. Concentrations of atomic species at the torch exit were determined from emission coefficients of various argon and oxygen (715.67, 844.65, 822.68 nm) atomic lines, and a  $H_{\beta}$  line assuming Boltzmann distribution of atomic level populations. To determine concentrations of atomic species downstream of the anode, we calculated tables of LTE composition as a function of temperature and mole fraction of entrained air assuming a homogeneous mixture of plasma components with a mole fraction of argon, taken as an average value of that measured at the torch exit. Then, the mole fraction of air was obtained from a measured average mole ratio of atomic nitrogen to argon. We used the following Ar I lines: 696.54, 706.72, 750.93, 826.45, 840.82, 842.46, and 852.14 nm; and N I lines: 742.36, 744.23, 818.64, 821.63, 824.24, 856.77, 859.4, and 862.92 nm. Spectroscopy measurements are described in more detail in [16].

Profiles of temperature, velocity and composition in downstream parts of the jet, where the temperature was lower, were performed using the enthalpy probe system TEKNA (Tekna Plasma Systems, Sherbrooke, Québec, Canada) connected with quadrupole mass spectrometer Balzers QMS

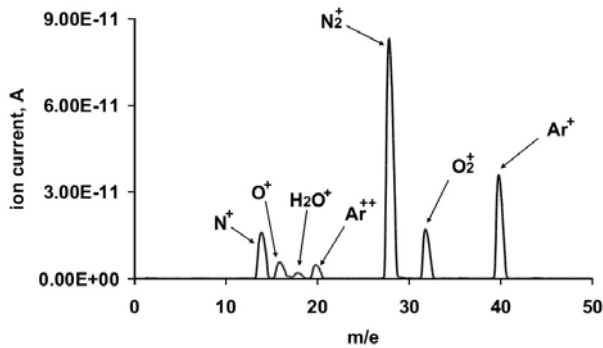


Fig. 3. Mass spectrum of plasma jet mixed with air at position 120 mm downstream of the jet axis.

200. The outer and inner diameters of the probe tip are 4.76 mm and 1.27 mm, respectively. The content of hydrogen and oxygen in the jet could not be measured directly because, after the recombination in the probe, water condenses in the enthalpy probe system. A freezer was used to prevent the influx of water into the TEKNA system. Real composition and properties of the plasma were then evaluated from measured data, assuming that the ratio of plasma gases (argon to steam) at a measured point is the same as the ratio at the nozzle exit determined by emission spectroscopy. Thus, the de-mixing of plasma components along the jet is neglected. The ratio of plasma to entrained air was determined from the ratio of argon concentration to nitrogen concentration. The example of a mass spectrum obtained by the mass spectrometer Balzers QMS 200 is shown in Fig. 3.

The velocity of the plasma flow in locations close to the nozzle exit, where an enthalpy probe could not be used

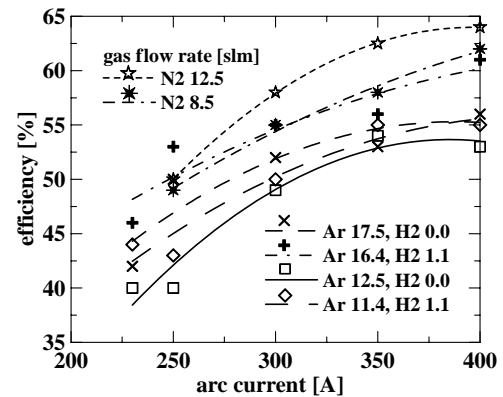
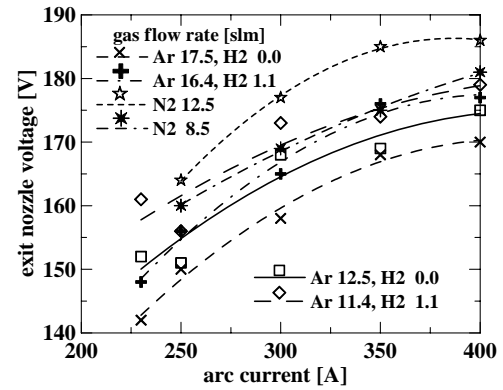
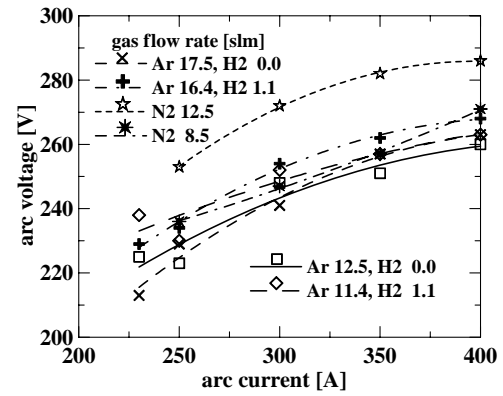


Fig. 4. Dependence of arc voltage, exit nozzle voltage (potential difference between cathode and exit nozzle) and efficiency  $\eta$  on arc current for argon, mixture of argon with hydrogen and for nitrogen.

because of high plasma temperatures, was determined from an analysis of fluctuations of light emitted by plasma. The plasma jet was imaged on an array of six photodiodes with maximum spectral sensitivity at 850 nm that was positioned parallel to the axis of the jet. The frequency bandwidth of diode amplifiers was 30 Hz to 50 MHz. The velocity of plasma flow was determined from the stream-wise and the counter-stream-wise velocity of propagation of shock waves that were initiated by anode breakdowns in a re-strike mode of anode attachment [17].

The images of the luminous plasma jet were obtained using a fast-shutter CCD camera from Sensicam Computer Optics.

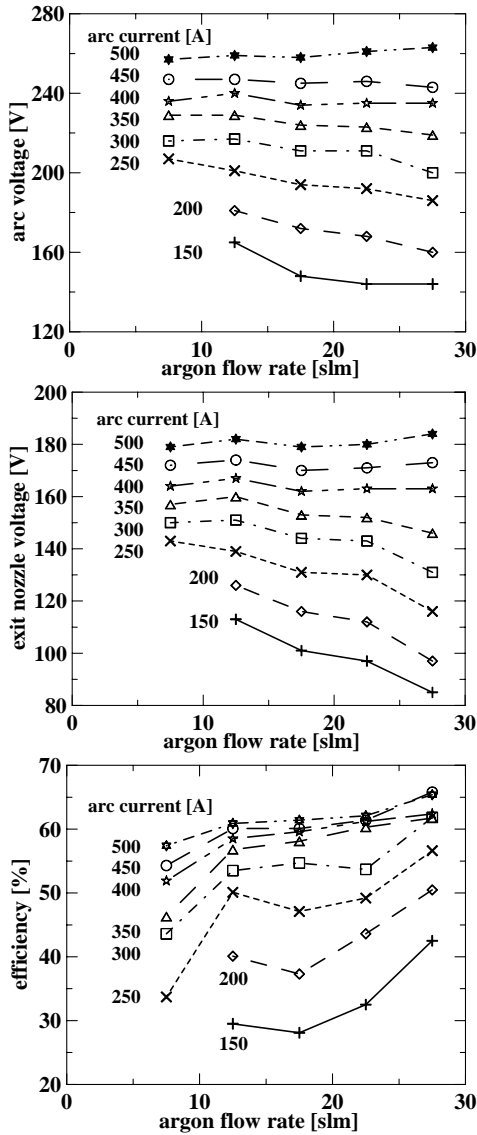


Fig. 5. Dependence of arc voltage, exit nozzle voltage and efficiency  $\eta$  on flow rate of argon for various arc currents.

From the images the shape of the jet was evaluated.

### III. EXPERIMENTAL RESULTS

Arc characteristics and jet properties were measured for arc currents of 200 A to 500 A, arc power levels of 40 kW to 133 kW, argon flow rates of 7 slm to 30 slm, nitrogen flow rates of 8.5 slm and 12.5 slm and mixture of argon with hydrogen (11.4/1.1 slm). Water evaporation rates were in the range of 0.2 g/s to 0.5 g/s.

#### A. Arc Characteristics and Power Balances

Volt-ampere characteristics of the whole arc, volt-ampere characteristics of the stabilized section of arc inside the arc chamber and the efficiency of the stabilized arc section are presented in Fig. 4. The efficiency is defined as a ratio of total enthalpy flux through the exit nozzle to power input into the stabilized part of the arc column inside the arc chamber. The

characteristics of the internal stabilized arc section were determined from the measured potential of the exit nozzle. If the resistance of the voltage divider was much greater than the resistance of the sheath between the arc column and the nozzle wall, the potential of the nozzle was equal to the potential of the arc column. The total arc voltage includes also the potential drop on the section of the arc in the free jet downstream of the exit nozzle. The power loss from this section of the arc column could not be measured. For some applications, the heat that is transferred from the outer section of the arc column can be used for materials treatment and thus the efficiency of the whole plasma torch is higher than the efficiency of the inner section of arc shown in Fig. 4. The measurements were performed for argon, mixtures of argon with hydrogen with the same total gas flow rates, and for nitrogen.

Volt-ampere arc characteristics increased for all gases in the range of currents from 250 A to 400 A, and the arc power varied from 50 kW to 114 kW. The voltage drop on the cathode gas-stabilized part of the arc column, determined from measurements of the potential of cathode nozzle, was in the range of 7 to 15 V; the power dissipated in this part of arc column was 1.8 to 6 kW and was in all cases substantially lower than the arc power. The efficiency increased as did the arc current. The highest voltage and efficiency were found for nitrogen; the addition of a small amount of hydrogen into argon resulted in an increase of both the arc voltage and efficiency.

The influence of the argon flow rate on arc characteristics can be seen in Fig. 5. For higher arc currents, both the arc voltage and the voltage drop on the stabilized part of the arc are almost independent of argon flow rate, whereas for lower

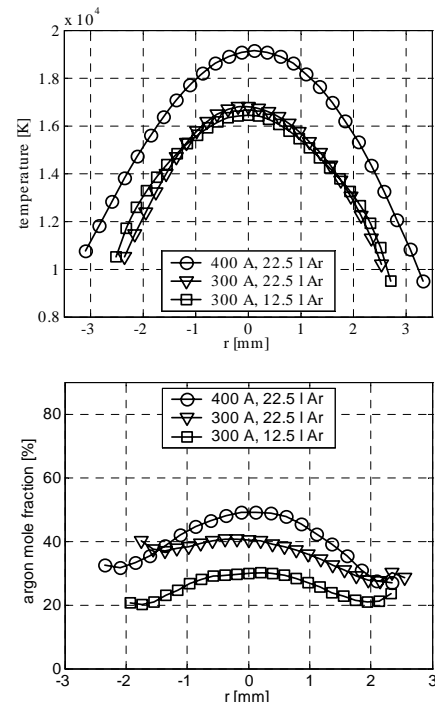


Fig. 6. Profiles of plasma temperature and argon molar fraction at the position 2 mm downstream of the torch exit for argon flow rates 12.5 and 22.5 slm for arc currents 300 A and 400 A.

currents the voltages and thus also arc power decrease with increasing gas flow rate. The efficiency of the internal section of arc increases if the argon flow rate is increased, for lower currents this dependency is steeper.

### B. Properties of Plasma Jet at the Nozzle Exit

Profiles of the plasma temperature and the composition as well as the plasma flow velocity were measured in the region

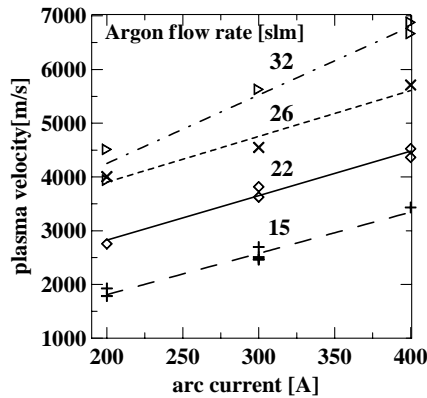


Fig. 7. Centerline plasma velocity in the anode region as a function of arc current for various argon flow rates.

just downstream of the nozzle exit. Fig. 6 reveals the results of diagnostics of the plasma jet at position 2 mm downstream of the nozzle exit by emission spectroscopy. Profiles of the plasma temperature and of the molar concentration of argon for arc currents of 300 A and 400 A for two argon flow rates

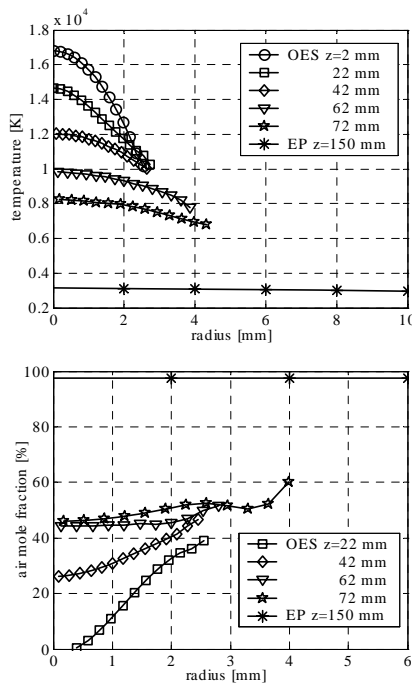


Fig. 8. Profiles of temperature and air mole fraction for various distances from the torch exit. Values for distances of 2 to 72 mm were obtained by emission spectroscopy values for 150 mm and were measured by enthalpy probe. Arc current 300 A, argon flow rate 22.5 slm.

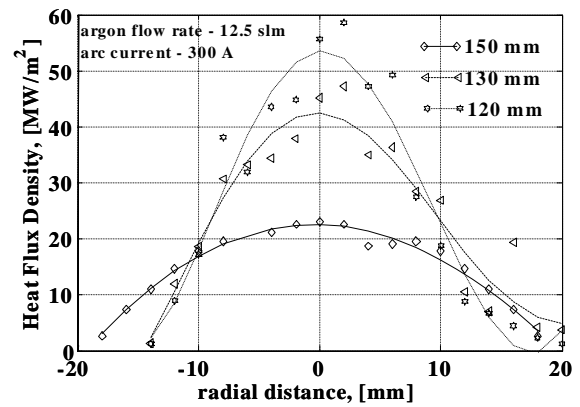


Fig. 9. Profiles of heat flux density at various distances from the nozzle exit. Arc current 300 A, argon flow rate 12.5 slm.

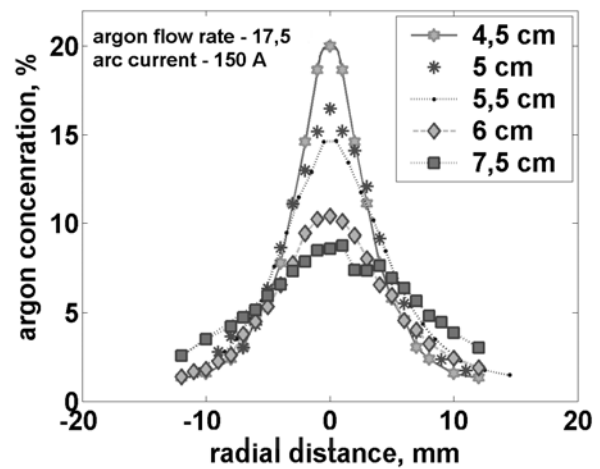


Fig. 10. Argon concentration profiles for various distances from the torch exit. Arc current 150 A, argon flow rate 17.5 slm.

are presented. As can be seen, the temperature profile is not affected by the change of argon flow rate from 12.5 slm to 22.5 slm. It is due to a great difference in enthalpies of argon and steam plasmas. The addition of argon with very low enthalpy does not influence much the energy balance of the arc, which is dominantly controlled by properties of steam plasma. The change of arc current from 300 A to 400 A resulted in a change of the axis temperature from 16,800 K to 19,200 K. These temperatures are about 2500 K lower than temperatures measured in a pure water torch with a similar configuration of the water-stabilized section [9].

Molar concentrations of argon in plasma leaving the nozzle were evaluated from measured emission coefficients of various argon and oxygen lines and from the  $H_{\beta}$  line. The concentration of argon has a maximum at the centerline of the jet as steam, flowing into arc column from the water walls that surrounds the arc in the water-stabilized section, and is not completely mixed with argon. In Fig. 6 the results of the measurement for arc currents 300 A and 400 A are presented.

Spectroscopic measurements were performed for arc currents of 150 A to 500 A and argon flow rates of 8 slm to 28

slm. Measured centerline temperatures varied between 14 000 K and 22 000 K, and argon molar concentrations were in the range of 20 to 80%.

Averaged values of the plasma flow velocity in the region from nozzle exit to 20 mm downstream of nozzle exit were evaluated from measurements of speed of propagation of disturbances in the plasma jet [17]. The dependence of the averaged velocity on the arc current for several argon flow rates is shown in Fig. 7. High velocities of up to 7 km/s were found. The velocity increases with an increase of both the arc current and the gas flow rate.

### C. Evolution of Plasma Properties along the Jet

The dependence of the plasma jet properties on the distance from the torch exit and the effect of the argon flow rate on the evolution of properties along the jet were studied by emission spectroscopy and enthalpy probe diagnostics. Because the torch is used for plasma spraying, the measurements were performed for distances up to 150 mm, where substrate is usually positioned.

Radial profiles of the temperature and the molar fraction of

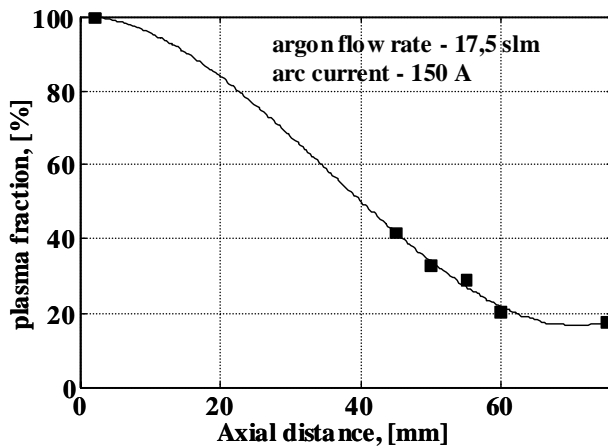


Fig. 11. Dependence of plasma fraction at the centerline of the jet on distance from the torch exit. Arc current 150 A, argon flow rate 17.5 slm.

air at several axial positions along the jet are shown in Fig. 8. Values marked as OES were obtained by emission spectroscopy; values marked EP were measured by the enthalpy probe. The decrease of temperature with increased distance from the torch exit, as well as the spread of the jet, are shown in the temperature profiles. Air concentration at the position 22 mm is zero at the jet centerline and increases at the jet fringes. Air reaches the jet centerline at a distance of between 22 mm and 42 mm. For longer distances the air concentration increases due to air entrainment and the profile of concentration is smoothed. At position 150 mm, the jet is composed almost exclusively of air at a temperature of about 3300 K and profiles of both the temperature and the air mole fraction are flat.

Heat flux profiles measured by an enthalpy probe at positions 120, 130 and 150 mm downstream of the nozzle exit are illustrated in Fig. 9. The jet is smoothed and the centerline

heat flux rapidly decreases as the distance from the torch exit increases. Unfortunately, the enthalpy probe diagnostics could not be applied for shorter distances from the torch exit because the probe tip would thereby be damaged.

The following two dependences were measured for a lower current of 150 A and an arc power of 30 kW to enable enthalpy probe diagnostics in positions close to the torch exit. Profiles of concentration of argon for several distances from

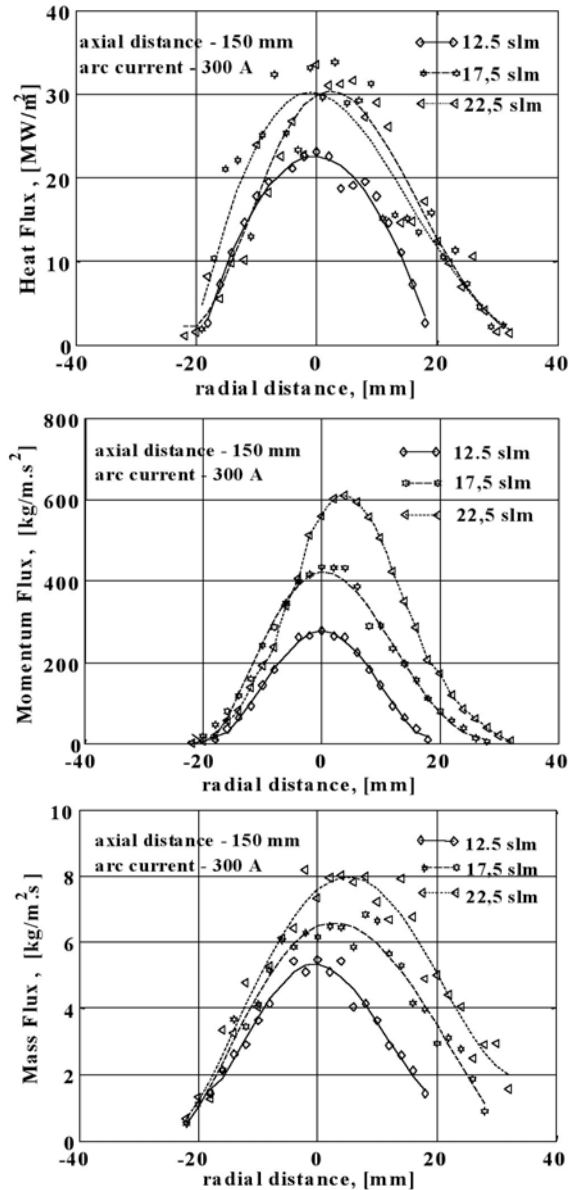


Fig. 12. Profiles of mass, momentum and heat fluxes at various flow rates of argon at position 150 mm downstream of the nozzle exit for an arc current of 300 A.

the torch exit in the region 45 to 75 mm are shown in Fig. 10. Air entrainment in this region can be evaluated from the reduction of argon concentration as the distance from the torch increases. The evolution of concentration of plasma gas components at the centerline position of the jet are shown in Fig. 11.

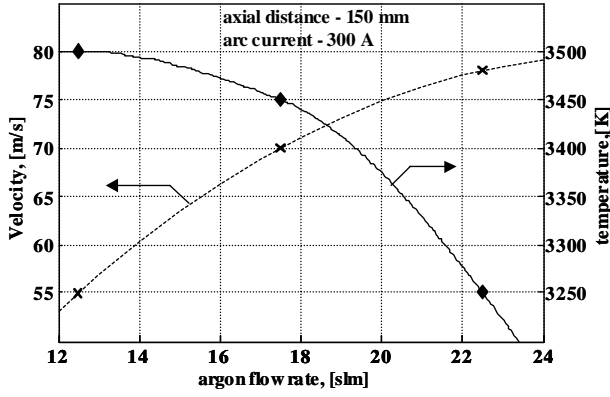


Fig. 13. Dependence of centreline velocity and temperature at axial position 150 mm on argon flow rate. Arc current 300 A.

TABLE I

TOTAL MASS, MOMENTUM AND ENTHALPY FLUXES THROUGH THE CROSS SECTION OF JET AT POSITION  $z = 150$  MM FOR THREE ARGON FLOW RATES AND SPREAD ANGLES OF THE JET.

Argon flow rate [slm]	Mass flux [g/s]	Momentum flux [kg.m/s <sup>2</sup> ]	Enthalpy flux [kW]	Spread angle [degrees]
12.5	3.5	0.13	16.0	6.4
17.5	7.4	0.29	30.4	8.3
22.5	10.6	0.42	29.8	9.5

#### D. Effect of Argon Flow Rate on Mass, Momentum and Heat Fluxes in the Jet

As can be seen in Figs. 6 and 7, changes of the argon flow rate result in a substantial change of the plasma flow velocity while the plasma temperature remained unchanged. In what follows, it will be seen how the change of the argon flow rate, i.e., the changes of plasma density and velocity at constant temperature, influences the mass, momentum and heat fluxes in the jet. The fluxes were measured by an enthalpy probe.

Fig. 12 shows measured radial profiles of mass, momentum and enthalpy fluxes at position 150 mm for an arc current of 300 A and three argon flow rates. All three fluxes increase due to the rise of the argon flow rate. The centerline velocity is increased and the centerline temperature is slightly reduced, as can be seen in Fig. 13.

Total mass, momentum and enthalpy fluxes were calculated by integration of the measured profiles in Fig. 12. The results are given in Table 1. Values of the jet spread angle, evaluated from the profiles of momentum flux, are also given in Table 1. Mass and momentum fluxes increase rapidly with increasing argon flow rate. This increase is steeper than an increase of plasma flow rate at the torch exit. Moreover, the enthalpy flux at a position 150 mm was increased due to the rise of argon flow rate from 12.5 slm to 17.5 slm, although the enthalpy flux at the torch exit was almost unchanged, as can be seen from values of arc voltage and efficiency in Fig. 5.

It seems that decreases of temperature and velocity along the jet due to the air entrainment and the turbulence are

reduced due to increasing argon flow rate, which leads to the increase of measured fluxes. This is confirmed also by the images of plasma jet at two argon flow rates that are shown in Fig. 14. The luminous jet core was prolonged due to the increase of argon flow rate while the total enthalpy flux at the nozzle exit was changed insignificantly – 14.4 kW at argon flow rate 12.5 slm and 14.5 kW at 22.5 slm.

#### IV. ANALYSIS OF THE RESULTS AND DISCUSSION

Arc characteristics are dominantly controlled by processes in the water-stabilized part of the arc column that is much longer than the cathode section and the section in a free jet. The effect of the gas flow rate on and the composition of arc properties can be analyzed on the basis of the following simple model of the water-stabilized section of the arc column. The conducting arc channel is represented by an isothermal cylinder of the length  $L$  and cross section  $A$ . The plasma from the cathode section enters axially the cylinder with the total flow rate  $G_0$ . Due to evaporation at the inner surface of the stabilizing water vortex, steam flows into the column radially with the flow rate per unit length  $m$ . The heat, dissipated in the column by Joule heating, is spent partially to heat inflowing steam to the temperature of the column, the fraction  $\alpha$  of the heat is transferred radially by heat conduction and radiation to the water vortex. Part of this radially transferred heat is absorbed in the steam flowing from the water surface. This part of the heat is returned back to the column. The absorption is represented by coefficient  $\varepsilon$ . Power balance in the conducting column can be written as

$$\frac{d(\rho v h A)}{dz} = IE - P, \quad (1)$$

where  $\rho$  is the plasma density,  $h$  is the enthalpy and  $v$  is the axial velocity,  $I$  is the arc current and  $E$  is the electric field intensity,  $P$  is the power loss to the stabilizing water vortex per unit length and  $z$  the axial coordinate. The power loss  $P$  includes the power transferred to the water and the power spent for water evaporation from the inner surface of the vortex. According to the assumptions specified above, the power loss can be expressed as

$$P = (1 - \varepsilon) \alpha I E. \quad (2)$$

The following relation between efficiency  $\eta$  and coefficients  $\alpha$  and  $\varepsilon$  that characterize radial heat transfer is obtained:

$$\eta = 1 - \alpha(1 - \varepsilon). \quad (3)$$

Equation (1) can be easily integrated if coefficients  $\alpha$ ,  $\varepsilon$  are supposed independent of  $z$ . After the substitution  $E = dU/dz$ , we can derive an equation for the voltage drop on a water stabilized arc column in the form:

$$U = \frac{(\rho v h A)_e}{\eta I}, \quad (4)$$

where  $(\rho v h A)_e$  is the total enthalpy flux at the nozzle exit. The total mass flow rate at the nozzle exit is

$$(\rho v A)_e = G_0 + m L. \quad (5)$$

Enthalpy of plasma created by mixture of gas with steam can be expressed as

$$h = \frac{G_0 h_{gas} + m L h_{H_2O}}{G_0 + m L}. \quad (6)$$

Equation (6) is valid with good accuracy for high temperatures in conducting the arc column where the effect of chemical reactions between gas and steam plasma on the enthalpy of mixture need not be considered.

The arc current is given by the equation

$$I = \sigma A E = \sigma A \frac{U}{L}. \quad (7)$$

The equation for a voltage drop on the water-stabilized part of arc column can be than written as

$$U = \left( \frac{L}{A \eta} \right)^{\frac{1}{2}} \left( G_0 \frac{h_{gas}}{\sigma} + m L \frac{h_{H_2O}}{\sigma} \right)^{\frac{1}{2}}. \quad (8)$$

All measured dependences of volt-ampere characteristics and efficiency on the composition of gas and the flow rate can be explained by differences in the contributions of individual heat transfer mechanisms that are caused by differences in material properties of steam, argon, hydrogen and nitrogen plasmas. The efficiency  $\eta$  given by (3) depends on coefficients  $\alpha$  and  $\varepsilon$  representing the relation between radial and axial heat transfer and intensity of heat absorption in the vapor, respectively. The arc voltage is determined by the value  $\eta$ , by the gas flow rate and the evaporation rate of steam and by the ratios of the enthalpies of gas components to the electrical conductivity of the gas/steam mixture.

The addition of argon into the arc chamber reduces the thermal conductivity of the mixture while radiation properties and absorption of radiation in the colder zones are affected only slightly. Consequently the radial heat transfer, described by coefficient  $\alpha$ , is reduced due to an increase of argon flow rate, while  $\varepsilon$  is not changed significantly. The reduction of  $\alpha$  is significant for lower currents when the heat conduction is the dominant mechanism of the radial heat transfer, whereas for higher currents the radiation component prevails and  $\alpha$  is

almost unchanged. Therefore, the efficiency  $\eta$  increases with increased argon flow rate at lower currents.

Because the enthalpy of argon plasma is one order lower than the enthalpy of steam plasma while the electric conductivity is changed only slightly with a change of content of argon in plasma, the effect of argon flow rate on the term in the second bracket of (8) is small. Thus, the arc voltage is decreased due to an increase of  $\eta$  and for the reasons given above this effect is significant at lower currents. The addition

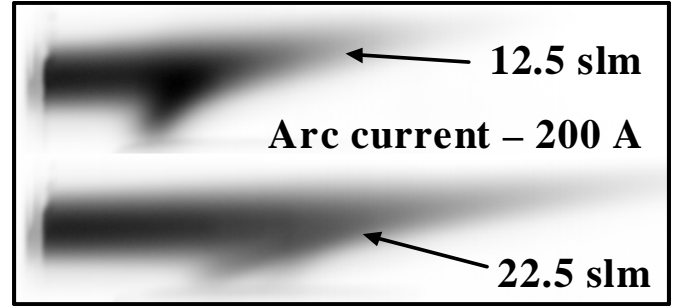


Fig. 14. Two images of luminous jet core with the anode attachment (on the bottom of the image) recorded by the fast shutter camera for flow rates of argon of 12.5 slm and 22.5 slm and arc current 200 A.

of argon into a water-stabilized arc does not influence significantly the enthalpy flux in the axial plasma flow and changes of the arc power are related primarily to changes of the radially transferred energy. Therefore, the plasma temperature and the total heat flux are almost constant while the mass flow rate and the plasma velocity are substantially increased due to an increase of argon flow rate, as can be seen in Figs. 6 and 7. Measured values of plasma velocity are substantially higher than the values achieved in the water-stabilized torch reported in [3]. The highest velocity, at an arc current of 400 A and an arc power of 94 kW, was almost 7 km/s (see Fig. 7) whereas for the water torch at 400 A and 107 kW the centerline velocity was 4.4 km/s [3].

The addition of hydrogen or nitrogen to the arc plasma affects not only radial heat transfer but also plasma enthalpy, because the enthalpy of nitrogen is comparable to the enthalpy of steam and the enthalpy of hydrogen is even higher. This leads to an increase of the arc voltage with increasing flow rates of hydrogen or nitrogen. At the same time, the efficiency is also increased due to an increase of  $\varepsilon$  because the addition of the molecular gases leads to an increase of the absorption in the arc fringes due to the photo-dissociation of ultraviolet radiation, which is intensive especially at higher currents. As the total enthalpy flux increases, the fraction of radially transferred arc power  $\alpha$  is decreased, resulting in an increase of efficiency.

The rise of the arc voltage and of efficiency with increasing arc current is caused by changes of the plasma composition due to the increased evaporation rate. A higher concentration of steam results in an increase of plasma enthalpy. Thus, the ratio  $\alpha$  of the heat transferred radially to the axial enthalpy



flux is reduced and consequently the efficiency  $\eta$  as well as the voltage  $U$  given by (3) and (8) are increased.

The plasma temperature profile in the jet is flattened as the distance from the nozzle exit increases, the axis temperature rapidly falls and the jet radius is increased. This is mainly caused by entrainment of the air into the jet. Because the flow velocity is high and the plasma density is much lower than the ambient air density, the air entrainment and the development of turbulence are intensive. At first the air concentration increases at the jet fringes. At the distances higher than 40 mm, relatively high air concentrations were found even in the jet centerline positions. For distances above 70 mm, the air concentration was 50% or more for arc currents of 150 A and 300 A. At the position 150 mm from the torch, the flowing medium contains more than 90% of air.

The influence of the argon flow rate on the evaporation rate of stabilizing water can be evaluated from the measured concentration of argon in the argon-steam plasma. On the assumption that the argon to steam concentrations ratio within the arc chamber is the same as measured concentrations at the nozzle exit, the evaluated values of evaporation rates were 0.5 g/s and 0.53 g/s for argon flow rates of 12.5 slm and 22.5 slm, respectively, at an arc current of 300 A. Thus, the evaporation rate was not significantly affected by the argon flow rate and total mass flow rate though the arc chamber was changed from 0.9 to 1.2 g/s if argon was increased from 12.5 slm to 22.5 slm. The plasma density was  $6.8 \text{ g/m}^3$  for 12.5 slm and  $9.6 \text{ g/m}^3$  for 22.5 slm in the centerline 2 mm downstream of the nozzle exit.

As Fig. 12 and Table 1 show, the mass and momentum fluxes, as well as the total mass and momentum fluxes, at the position 150 mm from the nozzle exit increase rapidly with an increase of the argon flow rate. At the same time, the dimensions of the luminous jet core and also the jet spread angle are increased. This is caused by an increase of the plasma density and the plasma flow velocity at the nozzle exit. Simultaneously, the plasma temperature and the heat flux through the nozzle remain almost unchanged. Thus, by changing the argon flow rate one can control the dimensions of the jet and the kinetic energy of flowing plasma while temperatures and heat fluxes remain constant. This may be advantageous in plasma spraying where heating and acceleration of injected powder particles could be controlled independently.

## V. CONCLUSIONS

The new-type hybrid water/argon plasma torch was derived from the water plasma torch, in which the arc was stabilized by a vortex of water. In the hybrid torch the arc chamber is divided into a short cathode part, where the arc is stabilized by a tangential gas flow with a vortex component, and a longer water-stabilized part. This arrangement not only provides additional stabilization of the cathode region and protection of the cathode tip, but also offers the possibility of controlling

the plasma jet characteristics in a significantly wider range than that of pure gas- or liquid-stabilized torches. In contrast to the gas torches, the hybrid torch is equipped with an external water-cooled rotating disc anode positioned a few mm downstream of the nozzle exit.

Characteristics of the torch and properties of plasma jet were measured for arc currents of 150 - 500 A, arc powers of 22 - 130 kW, and gas flow rates of 8 - 28 slm. Measurements of the arc characteristics were made for argon, mixtures of argon with hydrogen and for nitrogen. The effect of the gas flow rate and composition can be explained on the basis of a simple integral model of the hybrid arc. Enthalpy, thermal conductivity and radiation characteristics are decisive material properties that control arc and plasma parameters.

The influence of the gas flow rate on plasma jet properties was studied for argon. The volume percentage of argon in the plasma flow at the torch exit depends not only on the argon flow rate, but also on the arc current because the evaporation rate of the stabilizing water increases with an input power. The volume percentage of argon varied from 20 to 80%. The centerline plasma flow velocity close to the torch exit, increasing with both current and argon flow rate, ranges approximately from 1800 m/s to 7000 m/s. The exit temperature is almost independent of argon flow rate and varies between 14 000 and 22 000 K. The plasma temperatures were somewhat lower than those measured in water-stabilized torches; the plasma velocity was significantly higher. The jet spread angle as well as the mass and momentum fluxes in the downstream positions of the jet were substantially increased due to an increase of argon flow rate.

The torch affords the possibility of controlling plasma velocity and momentum flux in the plasma jet by changing the argon flow rate, almost independently of plasma temperature, which is determined by an arc current. In plasma spraying, it may be advantageous that heating and acceleration of injected powder particles be controlled independently.

Similar to water torches, the hybrid torches are characterized by high values of the arc voltage, high plasma temperatures and high plasma velocities. Thus, in plasma spraying, the torches exhibit performance characteristics typical for the water-stabilized torches, especially very high spraying rates and the ability for good melting of any sprayed material. The fields of application of the hybrid torches are thus large area coatings, powder treatment and spraying materials with high melting points.

## REFERENCES

- [1] E. Pfender, M. Boulos and P. Fauchais, *Thermal Plasmas Fundamentals and Applications*, New York-London: Plenum Press, 1994, ch. 1.
- [2] *Thermal Plasma Torches and Technologies*, vol. 1, O. P. Solonenko, Ed., Cambridge: Cambridge Int. Sci. Publ., 2001.
- [3] M. Hrabovsky, "Water-stabilized plasma generators," *Pure & Appl. Chem.*, vol. 70, pp. 1157-1162, 1998.
- [4] M. Hrabovsky, M. Konrad, V. Kopecky and V. Sember, "Properties of water stabilized plasma torches," in *Thermal Plasma Torches and Technologies*, vol.1, O.P. Solonenko, Ed., Cambridge: Cambridge Int. Sci. Publ., 2000, pp. 242-266.

- [5] F. Burnhorn and H. Maecker, "Electric field measurements in a water-stabilized high power arc," *Z. f. Phys.*, vol. 129, pp.369-376, 1951. in German.
- [6] R. W. Larentz, "Temperature measurements in a column of Gerdien arc," *Z. f. Phys.*, vol. 129, pp. 343-364, 1951. in German.
- [7] F. Burnhorn, H. Maecker and T. Peters, "Temperature measurements in water-stabilized high power arc," *Z. f. Phys.*, vol. 131, pp. 28-40, 1951. in German.
- [8] H. Maecker, "Electric arc for high powers," *Z. f. Phys.*, vol. 129, pp.108-122, 1951.
- [9] M. Hrabovsky, M. Konrad, V. Kopecky and V. Sember, "Processes and properties of electric arc stabilized by water vortex," *IEEE Trans. on Plasma Science*, vol. 25, pp. 833-839, October 1997.
- [10] M. Hrabovsky, M. Konrad, V. Kopecky and V. Sember, "Properties of electric arc stabilized by mixture of water with ethanol," *Annals New York Academy of Sciences*, vol. 891, pp. 57-63, December 1999.
- [11] J. Jeništa, "Water-vortex stabilized electric arc: I. Numerical model," *J. Phys. D: Appl. Phys.*, vol. 32, pp. 2763-2776, 1999.
- [12] J. Jeništa, "Water-vortex stabilized electric arc: II. Effect of non-uniform evaporation of water," *J. Phys. D: Appl. Phys.*, vol. 32, pp. 2777-2784, 1999.
- [13] P.Chraska and M. Hrabovsky, "An overview of water stabilized plasma guns and their applications," in *Proc. of Int. Thermal Spray Conf. & Exhib.*, Orlando, Florida, USA, 1992, pp. 81-86.
- [14] M. Hrabovsky, "Generation of thermal plasmas in liquid and hybrid DC arc torches," *Pure & Appl. Chem*, vol. 74, pp. 429-433, 2002.
- [15] M. Hrabovsky, M. Konrad, V. Kopecky, J. Hlina, J. Benes and E. Vesely, "Motion of anode attachment and fluctuations of plasma jet in dc arc plasma torch," *Journ. of High. Temp. Mat. Process*, vol. 1, pp. 167-178, 1997.
- [16] V. Sember, T. Kavka, V. Kopecky and M. Hrabovsky, "Comparison of spectroscopic and enthalpy probe measurements in H<sub>2</sub>O-Ar thermal plasma jet," in *Proc of Int. Symp. on Plasma Chemistry*, Taormina, Italy, June 2003.
- [17] M. Hrabovský, V. Kopecký, P. Macura: "Investigation of propagation of perturbations in thermal dc arc plasma jet," in *Progress in Plasma Processing of Materials 2001*. (ed. Pierre Fauchais). Begell House, New York – Wallingford (2001), 223–228.

**Milan Hrabovsky** received the M.Sc. degree in physics in 1967 and Ph.D. degree in plasma physics in 1975, both from the Faculty of Mathematics and Physics, Charles University, Prague. From 1967 to 1990, he was with the Institute of Electrical Engineering, Prague, where he was engaged in research on vacuum breakdown processes and physics of electric arcs in vacuum and gases as well as basic problems of current interruption and electromagnetic plasma launchers. In 1990 he joined Institute of Plasma Physics, Academy of Sciences of the Czech Republic, Prague, where he is currently head of the Department of Low Temperature Plasmas. His current research interests include physics of arc plasma torches, plasma chemistry and fundamentals of thermal plasma processing. Dr. Hrabovsky is a fellow of the International Union of Pure and Applied Chemistry, a member of the Board of Directors of International Plasma Chemistry Society and also of the Executive Committee of European Society of High Temperature Material Processes and a fellow of the Engineering Academy of the Czech Republic.

**Vladimír Kopecký** received his first degree in theoretical physics from the Faculty of Physics of the Moscow State University in 1963. He received the Ph.D. (CSc.) degree in physics in 1967 and the *Doctor Scientiarum* (DrSc.) degree in plasma physics in 1980. In 1963, he became a member of the scientific research staff of the Institute of Plasma Physics, Czechoslovak Academy of Sciences in Prague (since 1993 the Academy of Sciences of the Czech Republic, where he continues to work). He worked earlier in the field of instabilities in weakly and fully ionized plasmas, propagation, conversion and absorption of high-frequency waves in plasma, high-frequency heating of plasma and current drive in tokamaks. His current research interests since 1991 have been in thermal plasma generation in water stabilized plasma torches and their applications in plasma chemistry.

**Viktor Sember** received the M.S. degree in physics from the Faculty of Natural Sciences, T. G. Masaryk University, Brno, in 1985 and the PhD. degree in plasma physics from the Institute of Plasma Physics, Academy of Sciences of the Czech Republic, Prague, in 1999.

Since 1988, he has been a research worker at the Institute of Plasma Physics, Prague, Czech Republic. He has participated in several projects concerning generation and diagnostics of both thermal and non-equilibrium atmospheric plasmas for plasma chemical purposes. His current research interest is optical diagnostics of thermal plasmas and physics of thermal plasma jets.

**Oleksiy Chumak** received the B.S. and M.S. degrees in electronic systems from Sumy State University, Ukraine, in 2000. He is currently working toward the Ph. D. degree in the Thermal Plasma Department at the Institute of Plasma Physics, Academy of Science of the Czech Republic.

His research interests are the interaction between powder particles and plasma flow in plasma spraying technology as well as imaging diagnostics of plasma jet and powder particles behavior in the plasma spraying process.

**Tetyana Kavka** received the B.S. and M.S. degree in electronic system from Sumy State University, Ukraine, in 2000 and joined Charles University in the Czech Republic as Ph. D. student in plasma physics.

She has been with the Institute of Plasma Physics, Academy of Science of the Czech Republic since 2001. Her current research interests are processes of energy balances and heat transfer in arc plasma torches with gas and water stabilization and diagnostics of thermal plasma jets by the enthalpy probe.

**Milos Konrad** received the M.Sc. degree in physics in 1967 and RNDr. degree in physical electronics and optics in 1982, both from the Faculty of Mathematics and Physics, Charles University, Prague.

From 1967 to 1991, he was with the Institute of Electrical Engineering, Prague, where he was engaged in physics of electric arcs in vacuum and gases. In 1991 he joined Institute of Plasma Physics, Academy of Sciences of the Czech Republic, Prague. His current research interests include dc arc plasma torches and their applications.

Dr. Konrad is a member of European Society of High Temperature Material Processes.